Title

Selenium capped monolayer NbSe2 for two-dimensional superconductivity studies

Journal
physica status solidi (b), 253(12)

ISSN
0370-1972

Authors
Onishi, Seita
Ugeda, Miguel M
Zhang, Yi
et al.

Publication Date
2016-12-01

DOI
10.1002/pssb.201600235

Peer reviewed

Selenium capped monolayer $NbSe_2$ for two-dimensional superconductivity studies

Seita Onishi[1,5], Miguel M. Ugeda[1,†], Yi Zhang[2,3], Yi Chen[1], Claudia Ojeda-Aristizabal[1], Hyejin Ryu[2], Sung-Kwan Mo[2], Zahid Hussain[2], Zhi-Xun Shen[3,6], Michael F. Crommie[1,4,5] and Alex Zettl[1,4,5,*]

[1] Department of Physics, University of California at Berkeley, Berkeley, California 94720, USA.
[2] Advanced Light Source, Lawrence Berkeley National Laboratory, Berkeley, CA 94720, USA.
[3] Stanford Institute for Materials and Energy Sciences, SLAC National Accelerator Laboratory, Menlo Park, CA 94025, USA.
[4] Kavli Energy NanoSciences Institute at the University of California Berkeley and the Lawrence Berkeley National Laboratory, Berkeley, CA 94720, USA.
[5] Materials Sciences Division, Lawrence Berkeley National Laboratory, Berkeley, California 94720, USA.
[6] Geballe Laboratory for Advanced Materials, Departments of Physics and Applied Physics, Stanford University, Stanford, CA 94305, USA.
[†] Present address: CIC nanoGUNE, 20018 Donostia-San Sebastián, Spain

Received ZZZ, revised ZZZ, accepted ZZZ
Published online ZZZ (Dates will be provided by the publisher.)

Keywords monolayer niobium diselenide, superconductivity, molecular beam epitaxy, *in situ*

* Corresponding author: e-mail azettl@berkeley.edu, Phone: +01 510 642 4939, Fax: +01 510 643 8497

Superconductivity in monolayer niobium diselenide ($NbSe_2$) on bilayer graphene was studied by electrical transport. Monolayer $NbSe_2$ was grown on bilayer graphene by molecular beam epitaxy and capped with a selenium film to avoid degradation in air. The selenium capped samples have T_C=1.9K. *In situ* measurements down to 4K in ultrahigh vacuum show that the effect of the selenium layer on the transport is negligible. The superconducting transition and upper critical fields in air exposed and selenium capped samples were compared.

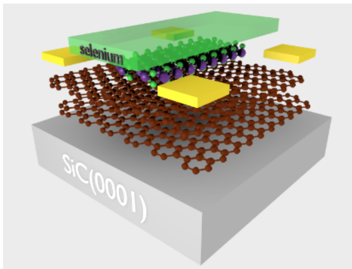

Schematic of monolayer $NbSe_2$/bilayer graphene with selenium capping layer and electrical contacts.

1 Introduction Interest in the layered compound, niobium diselenide ($NbSe_2$), has reemerged since the isolation of graphene from graphite [1]. $NbSe_2$ is abundant in phase transitions with a charge density wave state below 33K and superconductivity below 7.2K [2]. An early study on ultrathin $NbSe_2$ has observed a decrease in the critical temperature (T_C) of superconductivity as the layer number is reduced and predicted the monolayer T_C to be 3.8K from extrapolation [3]. Recently, both the charge density wave and the superconductivity in monolayer $NbSe_2$ have been investigated [4]–[7]. Although, there are discrepancies among observed monolayer T_C, they all fall below the extrapolated value of 3.8K. Remarkably, the upper critical field of monolayer $NbSe_2$ has been found to greatly exceed the Pauli paramagnetic limit for the field parallel to the layer [6].

In most studies on ultrathin $NbSe_2$, samples were prepared by mechanical exfoliation from bulk and capped with hexagonal boron nitride or graphene [4], [6]–[8]. Encapsulation of monolayer $NbSe_2$ is necessary because thin $NbSe_2$ has been known to degrade in air, possibly due to photo-oxidation [9]. In an alternate system, monolayer $NbSe_2$ has been grown by molecular beam epitaxy (MBE)

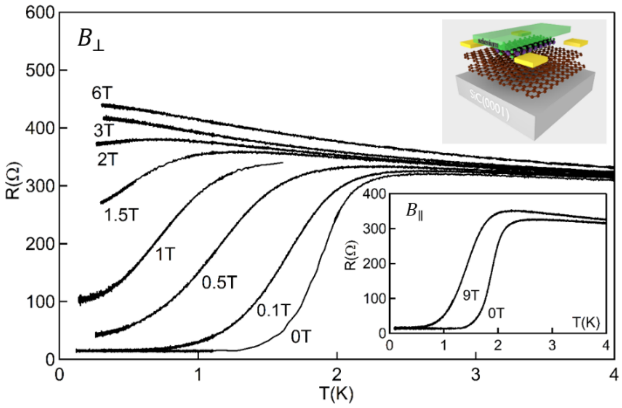

Figure 1 Resistance of selenium capped monolayer $NbSe_2$ (MBE)/bilayer graphene from 4K to 75mK. Each curve corresponds to the sample under a magnetic field in the direction perpendicular to the $NbSe_2$ layer ranging from 0T to 6T. Lower right inset: resistance of the same sample under a magnetic field in the direction parallel to the layer. The left curve corresponds to 9T and the right curve to zero field. Top right inset: schematic of the device structure.

on bilayer graphene and capped with a film of selenium [5]. The MBE prepared samples have a complimentary feature in that the selenium cap can be evaporated off to re-expose the surface. Surface sensitive techniques, such as scanning tunneling microscopy and photoemission have benefitted from the ability to expose the surface prior to an *in situ* study [5].

We have characterized the superconductivity in a MBE grown $NbSe_2$ on bilayer graphene by electrical transport down to 75mK and under magnetic fields up to 9T in the out-of-plane and in-plane directions. *In situ* studies at ultrahigh vacuum down to 4K show that the selenium cap does not significantly change the electron-phonon coupling of the material. In the absence of the selenium cap, brief exposure to air caused the T_C to go down and the transition to broaden. When the superconducting transitions in selenium capped and air exposed samples were normalized by their T_C, a large relative change above T_C and negligible change below T_C was observed. Furthermore, the upper critical fields (B_{C2}) perpendicular to the layer were compared. As expected, the air exposed sample has a significantly lower B_{C2}. Even after rescaling the temperature dependence of B_{C2} by the reduction in T_C, the rescaled B_{C2} behavior was still suppressed compared to the selenium capped sample.

2 Results The device shown by the schematic in the inset of Figure 1 was prepared as previously reported [5]. Bilayer graphene was grown epitaxially on silicon carbide and monolayer $NbSe_2$ was grown by MBE on top of the bilayer graphene. A selenium capping layer was deposited *in situ* to cover the $NbSe_2$ portion. Contacts were deposited on the areas of exposed graphene and the DC resistance of the sample was measured in a four-point probe configuration. Figure 1 shows the temperature dependence of the resistance. The sharp drop in resistance indicates a superconducting transition. We define T_C as the resistive midpoint. Without magnetic field, the sample resistance starts to deviate from normal state behavior at the onset temperature T_{onset}=2.6K. The resistance reaches half of the normal state value at T_C=1.9K and flattens out to a value close to zero at T_{zero}=1.3K. The finite resistance below T_{zero} is sample dependent and values much closer to zero were observed in other samples. Previously reported T_C for thin $NbSe_2$ by Cao et al. and Xi et al. are in agreement for multi-layers down to bilayers but show discrepancy for the monolayer [6], [7]. Our results are consistent with T_C~2K reported by the former.

As expected of superconductivity, the T_C shifts to lower temperatures under a magnetic field. As shown in Figure 1, when the magnetic field is perpendicular to the $NbSe_2$ layer, signatures of superconductivity disappear for fields above 3T. The curves for 3T and 6T show thermally activated behavior of an insulator, which is consistent with the superconductor-insulator transition for two-dimensional superconductivity [10], [11]. For the superconducting transition at $B_\perp$=1T below T_C, the resistance starts to plateau at a larger finite value. While an intermediate metallic state in the superconductor-insulator transition has been reported for bilayer $NbSe_2$, it has not been observed in monolayer $NbSe_2$ [8]. For our system, further studies are needed to rule out other sources of finite resistance. As shown in the inset of Figure 1, superconductivity still persists at 9T when the magnetic field is parallel to the $NbSe_2$ layer. The upper critical field is much higher than 9T for parallel fields. Although the fields were not high enough to confirm the unusually high upper critical field in monolayer $NbSe_2$, the anisotropy is consistent with a thin film superconductor [6], [12].

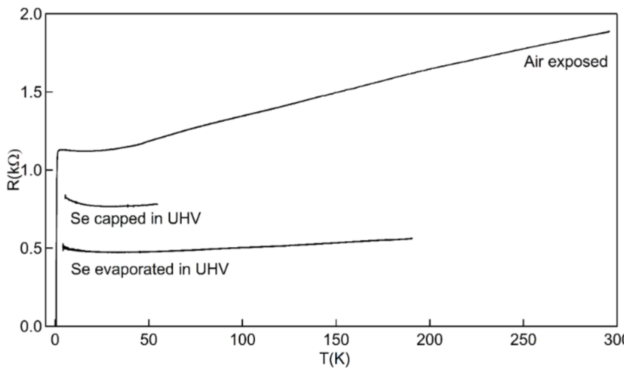

Figure 2 Comparison of monolayer $NbSe_2$ (MBE)/bilayer graphene resistance with and without selenium cap in the 4K to 50K range. Lower curve corresponds to the *in situ* sample measurement in UHV after selenium cap was evaporated. Middle curve corresponds to the sample measurement in UHV prior to selenium cap evaporation. Upper curve corresponds to the sample measurement after a brief air exposure in the absence of a selenium cap.

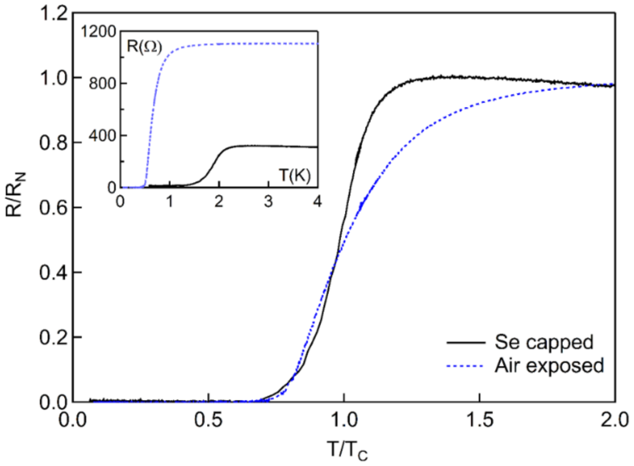

Figure 3 Rescaled superconducting transition of selenium capped and air exposed monolayer $NbSe_2$ (MBE)/bilayer graphene. For each sample, the resistance was divided by R_N, the normal state value at T_{onset}, and the temperature was divided by T_C. The solid black line corresponds to the selenium capped sample and the dotted blue line corresponds to the air exposed sample. Top left inset: the resistance measurement data prior to rescaling.

To demonstrate that the selenium capping layer has negligible effect on the superconductivity in $NbSe_2$, electrical transport was compared in ultrahigh vacuum (UHV). As shown in Figure 2, the sample was first measured with the selenium capping layer intact down to 4K. Subsequently, the selenium film was evaporated in UHV and the resistance was measured again down to 4K. Although the sample resistance decreased, the temperature dependence of the resistance remains the same before and after the selenium evaporation. Hence, the electron-phonon coupling is unaffected by the presence of the selenium capping layer. The sample was briefly exposed to air during a rapid transfer to a different cryostat for measurements at lower temperatures. However, the sample remained metallic and a sharp drop in resistance due to superconductivity can be seen.

As shown in Figure 3, air exposure depressed the T_C to 0.65K and transition broadened to span from T_{onset}=1.9K to T_{zero}=0.46K. To compare the superconducting transitions of the selenium capped and air exposed samples, the temperature for each curve was rescaled by their respective T_C's and the resistance was normalized to the resistance at T_{onset}. Above T_C, Figure 3 shows significant broadening of the transition for the air exposed sample. The selenium capped sample reaches normal state behavior above T/T_C=1.4, whereas the air exposed sample is still undergoing transition. Surprisingly, there is little difference in the transition behavior between the selenium capped sample and air exposed sample below T_C. In a superconducting transition, the portions above and below T_C are governed by two different processes [13], [14]. In cooling from the normal state to T_C, the fluctuation of the superconducting order parameter induce excess conductivity and lowers the resistance from the normal state [15]. When approaching T_C from T_{zero}, the vortex dynamics induce finite resistance from phase slip events [16]. Figure 3 shows that degradation in air impacts the fluctuation enhanced conductivity regime above T_C more heavily than the phase slippage regime below T_C. Two-dimensional superconductor behavior has been confirmed in monolayer $NbSe_2$ in both above T_C with the Aslamazov-Larkin formula and below T_C by the extraction of Berezinskii-Kosterlitz-Thouless temperature [6]. Given that a quantum metal state has been observed in bilayer $NbSe_2$ below T_C, it is interesting that superconductivity is preferentially protected below T_C from disorder in monolayer $NbSe_2$ [8].

Figure 4 shows the temperature dependence of the upper critical field of the selenium ($B_{C2}(T)$) capped and air exposed sample for the field perpendicular to the $NbSe_2$ layer. The selenium capped sample extrapolates to $B_{C2}(0)$=1.3T at zero temperature. The decrease in slope at low temperature is consistent with bulk $NbSe_2$ behavior [17]. For the air exposed sample, the upper critical field is diminished to $B_{C2}(0)$=0.2T. To compare both samples, $B_{C2}(T)$ was normalized by the Pauli paramagnetic limit B_P=1.84T_C and the temperature was divided by T_C as shown in the inset of Figure 4 [18], [19]. Even after rescaling to account for the reduction in T_C, upper critical field behavior is more suppressed for the air exposed sample. The reduction in $B_{C2}(T)$ is more dramatic than if it were caused solely by the shift in T_C.

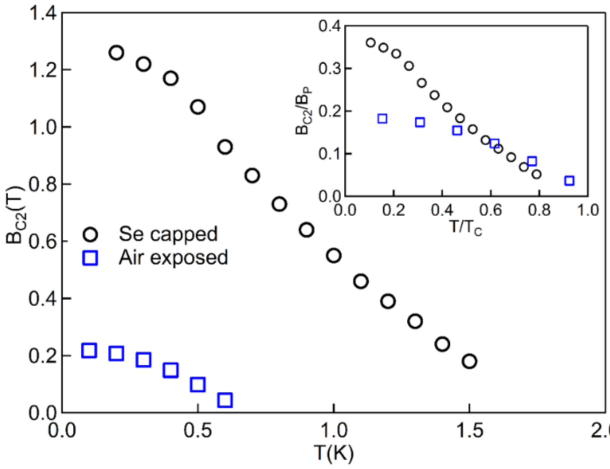

Figure 4 Upper critical field (B_{C2}) of selenium capped and air exposed monolayer $NbSe_2$ (MBE)/bilayer graphene from 75mK to 1.5K. Black circles correspond to the selenium capped sample and the blue squares correspond to the air exposed sample. Top right inset: the data with the B_{C2} rescaled by the Pauli paramagnetic limit $B_P = 1.84T_C$ and the temperature rescaled by T_C.

3 Conclusion When protected by a selenium capping layer, we have found the MBE grown monolayer $NbSe_2$ on bilayer graphene is stable in air. The system displays superconducting behavior, which is consistent with earlier studies on exfoliated $NbSe_2$ and the selenium capping layer does not affect the electron-phonon coupling of monolayer $NbSe_2$. Comparison of selenium capped and air exposed samples reveal that air exposure broadens the fluctuation enhanced conductivity regime above T_C. However, the T_C normalized temperature dependence of resistance in both samples remain the same in the phase slippage regime below T_C. Air exposure also suppresses the upper critical field of $NbSe_2$ by more than the effects due to the reduction of T_C.

Acknowledgements Research supported in part by the Director, Office of Energy Research, Materials Sciences and Engineering Division, of the US Department of Energy (DOE), under grant DE-AC02-05CH11231 supporting the sp2-bondedMaterials Program (magneto-transport), and by the National Science Foundation under award # DMR-1206512 (UHV transport).Work at the ALS is supported by DOE BES under Contract No. DE-AC02-05CH11231. H.R. acknowledges support from Max Planck Korea/POSTECH Research Initiative of NRF, Korea. M.T.E. is supported by the ARC Laureate Fellowship project (FL120100038). A.R. acknowledges fellowship support by the Austrian Science Fund (FWF): J3026-N16.

References

[1] K.S. Novoselov, D. Jiang, F. Schedin, T.J. Booth, V. V Khotkevich, S. V Morozov, and a K. Geim, Proc. Natl. Acad. Sci. U. S. A. **102**, 10451 (2005).
[2] J.M.E. Harper, T.H. Geballe, and F.J. Di Salvo, Phys. Lett. A **54A**, 27 (1975).
[3] R. Frindt, Phys. Rev. Lett. **28**, 299 (1972).
[4] X. Xi, L. Zhao, Z. Wang, H. Berger, L. Forró, J. Shan, and K.F. Mak, Nat. Nanotechnol. **10**, 765 (2015).
[5] M.M. Ugeda, A.J. Bradley, Y. Zhang, S. Onishi, Y. Chen, W. Ruan, H. Ryu, M.T. Edmonds, H. Tsai, and A. Riss, Nat. Phys. **12**, 92 (2016).
[6] X. Xi, Z. Wang, W. Zhao, J.-H. Park, K.T. Law, H. Berger, L. Forró, J. Shan, and K.F. Mak, Nat. Phys. **12**, 139 (2016).
[7] Y. Cao, A. Mishchenko, G.L. Yu, E. Khestanova, A.P. Rooney, E. Prestat, a V Kretinin, P. Blake, M.B. Shalom, C. Woods, J. Chapman, G. Balakrishnan, I. V Grigorieva, K.S. Novoselov, B. a Piot, M. Potemski, K. Watanabe, T. Taniguchi, S.J. Haigh, a K. Geim, and R. V Gorbachev, Nano Lett. **15**, 4914 (2015).
[8] A.W. Tsen, B. Hunt, Y.D. Kim, Z.J. Yuan, S. Jia, R.J. Cava, J. Hone, P. Kim, C.R. Dean, and A.N. Pasupathy, Nat. Phys. **12**, 208 (2016).
[9] M.S. El-Bana, D. Wolverson, S. Russo, G. Balakrishnan, D.M. Paul, and S.J. Bending, Supercond. Sci. Technol. **26**, 125020 (2013).
[10] A.M. Goldman, Phys. E Low-Dimensional Syst. Nanostructures **18**, 1 (2003).
[11] D.B. Haviland, Y. Liu, and A. M. Goldman, Phys. Rev. Lett. **62**, 2180 (1989).
[12] M. Tinkham, Introduction to Superconductivity: Second Edition (Dover Books on Physics) (Vol I), Second Edi (Dover Publications, 2004).
[13] W.J. Skocpol and M. Tinkham, Reports Prog. Phys. **38**, 1049 (1975).
[14] M.R. Beasley, J.E. Mooij, and T.P. Orlando, Phys. Rev. Lett. **42**, 1165 (1979).
[15] X.-D. Xiang, J.G. Hou, V.H. Crespi, A. Zettl, and M.L. Cohen, Nature **361**, 54 (1993).
[16] B.M. Kessler, Ç.Ö. Girit, A. Zettl, and V. Bouchiat, Phys. Rev. Lett. **104**, 047001 (2010).
[17] A. Nader and P. Monceau, Springerplus **3**, 16 (2014).
[18] B.S. Chandrasekhar, Appl. Phys. Lett. **1**, 7 (1962).
[19] A.M. Clogston, Phys. Rev. Lett. **9**, 266 (1962).